Available online at www.sciencedirect.com
ScienceDirect
Developmental Biology 317 (2008) 83–94
DEVELOPMENTAL BIOLOGY
www.elsevier.com/developmentalbiology

Canonical WNT/β-catenin signaling is required for ureteric branching

Darren Bridgewater [a,b], Brian Cox [a], Jason Cain [a,b], Agnes Lau [a], Valerie Athaide [a], Paul S. Gill [a,c], Satu Kuure [d], Kirsi Sainio [d], Norman D. Rosenblum [a,b,c,*]

[a] Program in Developmental and Stem Cell Biology, The Hospital for Sick Children, 555 University Avenue, Toronto, Ontario, Canada M5G 1X8
[b] Division of Nephrology, The Hospital for Sick Children, 555 University Avenue, Toronto, Ontario, Canada M5G 1X8
[c] Department of Physiology, and Laboratory Medicine and Pathobiology, University of Toronto, Canada
[d] Biochemistry and Developmental Biology, Institute of Biomedicine, University of Helsinki, Finland

Received for publication 16 November 2007; revised 30 January 2008; accepted 5 February 2008
Available online 21 February 2008

Abstract

WNT/β-catenin signaling has an established role in nephron formation during kidney development. Yet, the role of β-catenin during ureteric morphogenesis in vivo is undefined. We generated a murine genetic model of β-catenin deficiency targeted to the ureteric bud cell lineage. Newborn mutant mice demonstrated bilateral renal aplasia or renal dysplasia. Analysis of the embryologic events leading to this phenotype revealed that abnormal ureteric branching at E12.5 precedes histologic abnormalities at E13.5. Microarray analysis of E12.5 kidney tissue identified decreased *Emx2* and *Lim1* expression among a small subset of renal patterning genes disrupted at the stage of abnormal branching. These alterations are followed by decreased expression of genes downstream of *Emx2*, including *Lim1*, *Pax2*, and the ureteric tip markers, *c-ret* and *Wnt 11*. Together, these data demonstrate that β-catenin performs essential functions during renal branching morphogenesis via control of a hierarchy of genes that control ureteric branching.

Keywords: β-Catenin; Kidney development; Branching morphogenesis; WNT signaling; Canonical signaling; Microarray; *Emx2*

Introduction

Branching morphogenesis, defined as growth and branching of epithelial tubules during embryogenesis, is critical to the formation of organs including the kidney, lung, and mammary glands. In each organ, a multi-branched epithelial tree develops from unbranched epithelial progenitors in response to signals elaborated from adjacent mesenchymal tissue. Formation of the mammalian permanent kidney (metanephros) begins with the emergence of the ureteric bud as an epithelial outgrowth of the Wolffian duct in response to the adjacent metanephric mesenchyme. The ureteric bud invades the metanephric mesenchyme and gives rise to successive generations of ureteric bud branches that differentiate into the collecting ducts. In reciprocal fashion, metanephric mesenchyme cells adjacent to ureteric bud tips undergo a series of morphologic transitions whereby the epithelial elements of the nephron are formed (Saxen, 1987).

The stereotypic pattern of collecting duct and nephron formation suggests that the embryologic events giving rise to these structures are tightly regulated. Yet, the signaling mechanisms that control branching morphogenesis during mammalian kidney development (reviewed in Vainio and Lin, 2002) are not completely defined. β-Catenin is a bifunctional protein involved in cell–cell adhesion via adherens junctions, and in gene transcription as a critical effector in the canonical WNT pathway. Members of the WNT family of secreted glycoproteins control tissue patterning during vertebrate embryogenesis (Nusse, 2005). WNT signaling regulates cell functions by activating the canonical β-catenin pathway, the planar cell polarity pathway or the calcium pathway. WNT signals control levels of cytosolic β-catenin by inhibiting Glycogen Synthase Kinase (GSK) 3β-dependent β-catenin phosphorylation and subsequent proteasomal degradation of β-catenin. Inhibition of GSK3β

* Corresponding author. Division of Nephrology, The Hospital for Sick Children, 555 University Avenue, Toronto, Ontario, Canada M5G 1X8. Fax: +1 416 813 5252.
E-mail address: norman.rosenblum@sickkids.ca (N.D. Rosenblum).

0012-1606/$ - see front matter.
doi:10.1016/j.ydbio.2008.02.010

allows accumulation of β-catenin, which causes its nuclear translocation. In the nucleus, β-catenin regulates target gene expression in partnership with members of the Leukemia and the T Cell Factor (LEF/TCF) family (Huelsken and Behrens, 2002). The expression of *Wnt6, Wnt7b, Wnt9b and Wnt11* in the ureteric bud is consistent with a functional role for these WNTs during ureteric branching. Expression of β-catenin-dependent reporter genes in the Wolffian Duct and ureteric bud in transgenic mice suggests that WNTs can signal via the canonical pathway during branching morphogenesis (Maretto et al., 2003; Moriyama et al., 2007). While analysis of mice with β-catenin deficiency or over expression in nephron progenitors demonstrates an important role β-catenin during nephrogenesis (Park et al., 2007), the role of β-catenin and canonical Wnt signaling during ureteric branching is not defined.

Here, we demonstrate an essential role for β-catenin during renal branching morphogenesis. *Cre*-mediated inactivation of β-catenin targeted to ureteric cells disrupts branching morphogenesis and causes renal aplasia or dysplasia. Genome-wide analysis of mRNA expression and in situ mRNA hybridization in mutant and wild type kidney tissue demonstrated that decreased ureteric branching observed during the early stage of renal malformation in β-catenin mutant mice is accompanied by decreased *Emx2* and *Lim1* expression. These changes are followed by decreased expression of *Pax-2* and *c-ret* and the c-ret-dependent gene, *Wnt11*. Together, these data demonstrate that β-catenin acts upstream of a hierarchy of genes required for ureteric branching.

Materials and methods

Mice

Mice with a β-catenin allele containing LoxP sites flanking exons 2 through 6 (Brault et al., 2001) were crossed to *Hoxb7-Cre:Gfp* mice (Zhao et al., 2004) to generate *Hoxb7-Cre,Gfp*; *β-catenin* deficient mice. PCR genotyping was performed as described (Brault et al., 2001). TCF- and BAT-gal reporter mice (Cheon et al., 2002; Maretto et al., 2003) were used to determine β-catenin transcriptional activation. β-Galatosidase staining was performed as previously described (Godin et al., 1998).

Histology and immunohistochemistry

Paraffin-embedded embryos were analyzed by histology after generating 4 μm tissue sections and staining with haematoxylin and eosin. Anti-β-catenin C-18 (1:200 dilution, Santa Cruz, USA), and E-cadherin (1:100 dilution, Zymed, USA) immunohistochemistry was performed on formalin-fixed, paraffin-embedded kidney sections as previously described (Hu et al., 2003). Immunofluoresence was performed using anti-β-catenin (1:100 dilution) (Upstate, Lake Placid, USA) and anti-calbindin (1:200 dilution) (Sigma). Whole mount immunofluoresence was performed as described (Kuure et al., 2005) with DBA lectin (Vector Laboratories; 1:200) to identify the stalk epithelium (Michael et al., 2007). Alexa 568 and Alexa 488 (1:500 dilution) were used as secondary antibodies (Invitrogen, St. Louis, USA).

Microarray analysis

Kidneys from mutant mice were divided into three random pools ($n=3$) consisting of 6 kidneys each, while those from wild type mice were divided into 3 pools ($n=3$) consisting of 3 kidneys each. Kidneys were stored in RNAlater RNA stabilization reagent (Qiagen) and RNA was then isolated using the RNeasy micro kit (Qiagen). This provided sufficient RNA (1 μg total RNA) for a one cycle amplification. Microarray data was processed using GCOS (v1.4, Affymetrix). All CHIPS were scaled to a target value of 500 prior to expression analysis. Two wild type replicates were normalized to a third wild type replicate and these were used as baselines to normalize and compare the three replicate β-catenin deficient samples. Comparisons were made in all combinations to create a matrix of 3×3 crosswise comparisons (9 in total). Probe sets with present calls in all replicates in either the β-catenin deficient or wild type samples were kept and all others were removed from the data set. Probe sets with a significant change call in 6 of 9 comparisons were considered significantly changed in the β-catenin deficient versus wild type samples. To minimize the false positives a threshold signal log ratio (SLR) value was determined by estimating the background error using the distribution of SLR for probe sets with no significant change calls.

Gene ontology analysis

Probe sets were mapped to their gene symbol identifiers from annotation tables supplied by Affymetrix (http://www.affymetrix.com). Lists of gene symbols were entered into the BINGO plugin [v2.0 (Maere et al., 2005)] for Cytoscape [v 2.4 (Shannon et al., 2003)] and compared to Gene Ontology (GO) annotation tables from MGI (http://www.informatics.jax.org/) to calculate the enrichment of terms and their *P*-value, which was then adjusted by the Benjamini Hochberg correction for the false discovery rate (Hochberg and Benjamini, 1990). All reported enrichments were at a significance of 0.05 or less.

Real-time reverse transcriptase-PCR

Real-time PCR Amplification was performed using the Applied Biosystems 7900HT fast RT-PCR system. cDNA was generated using first strand cDNA synthesis (Invitrogen) from total RNA. Real-time PCR reaction mix contained 3 ng of each cDNA sample, SYBR green PCR Master Mix (Applied Biosystems) and 300 nM of each primer to a total volume of 25 μl. Primers for *Emx2*, *Lim1*, *c-ret*, *Wnt11*, *Pax2*, *myogenin*, and *E-cadherin* were designed using Primer 3 software and verified using the UCSC genome bioinformatics web site (genome.ucsc.edu). Primer design was very restrictive — the annealing temperature was restricted to 59–60 °C and the length of the PCR product was set between 100 and 200 bp. Specificity of the amplification was carried out by agarose gel electrophoresis. Relative levels of mRNA expression were carried out using the standard curve method. Individual expression values were normalized by comparison to β-2-microglobin.

Electron microscopy

Kidneys were fixed in 2% glutaraldehyde (GA) for 24 h, rinsed with 0.1 M sodium cocadylate and fixed for 1 h in 0.2% tannic acid followed by graded fixation in 1% osmium tetroxide and in 1% osmium tetroxide/1.25% potassium ferrocyanide. After dehydration samples were embedded in SPURR resin, sectioned, collected on copper grids and stained for EM. Images were obtained using a FEI Tecnai 20 transmission electron microscope.

In situ mRNA hybridization

Non-radioactive in situ hybridization was performed using DIG-labeled cRNA probes encoding *Emx2*, *Lim1*, *Pax-2*, *c-ret*, *GDNF, Wnt 11* on paraffin-embedded kidney tissue fixed with 4% PFA for 24 h at 4 °C as previously described (Mendelsohn et al., 1999).

In situ TUNEL assay, BrdU incorporation and data analysis

Terminal deoxynucleotidyl transferase (TdT)-mediated dUTP nick end labeling (TUNEL) was performed using 4% PFA fixed paraffin-embedded tissue sections as described in the manufacturer's instructions (Promega, Madison, WI). Cell proliferation was assayed in paraffin-embedded kidney tissue by incorporation of 5-bromo-2-deoxyuridine (BrdU, Roche Molecular Biochemicals, Mannheim, Germany), as described (Cano-Gauci et al., 1999). Pregnant

females received an intraperitoneal injection of BrdU (100 mg/g of body weight) 2 h prior to sacrifice. BrdU-positive cells were identified using an anti-BrdU peroxidase-conjugated antibody as described (Boehringer, Mannheim). Immunoreactivity was visualized using Aminoethyl Carbazole horseradish peroxidase chromogen/substrate solution (Zymed Laboratories, USA). Mean differences were examined by using Student's *t*-test (two tailed) and a Prism 3.0 statistics program. A difference of 5% was interpreted as being statistically significant.

Results

Deficiency of β-catenin in ureteric cells causes renal agenesis/hypodysplasia

We initiated investigation of β-catenin functions by determining whether it is expressed in a temporal and spatial pattern consistent with a functional role during branching morphogenesis. β-Catenin protein, identified by immunohistochemistry, was localized to both ureteric bud branches and nephrogenic intermediate structures in a pattern consistent with expression in adherens junctions (Figs. 1A, B). Since β-catenin also acts as a transcriptional co-activator, we next determined its potential to regulate transcription in the ureteric bud and its branches. Strong β-catenin-dependent expression of a β-galactosidase reporter gene was detected in the epithelium of the branching ureter of TCF-gal reporter mice (Cheon et al., 2002) (Fig. 1C). A similar pattern of expression was detected in the kidneys of BAT-gal reporter mice (Maretto et al., 2003) (Fig. 1D). Together, these data suggest a role for β-catenin in regulating gene transcription during branching morphogenesis.

Homozygous germline deficiency of β-catenin in the mouse results in embryonic lethality prior to the onset of kidney development. Accordingly, we generated mice in which β-catenin deficiency is targeted to ureteric cells by crossing mice which contain a β-catenin floxed allele (Brault et al., 2001) to mice that express *Cre-recombinase* under the control of a *Hoxb7*-promoter (Kress et al., 1990; Srinivas et al., 1999). Deficiency of β-catenin in ureteric cells was demonstrated by immunohistochemistry in E13.5 kidney tissue (Figs. 1E, F). As expected, β-catenin was expressed in the ureteric bud and developing nephron structures in *Wt* mice (Fig. 1E). In contrast, in β-catenin deficient mice expression of β-catenin was not detected in ureteric bud derived structures, but was expressed in metanephric mesenchyme (Fig. 1F). We confirmed the deficiency of β-catenin in ureteric cells by co-localizing β-catenin and calbindin-D28K, a marker of ureteric cells, using immunofluoresence microscopy (Figs. 1G–L). In kidney tissue isolated from wild type mice, β-catenin co-localized with calbindin in ureteric epithelium, and was also detected in calbindin-negative tubules and mesenchymal cells (Figs. 1G–I). In contrast, β-catenin expression was undetectable in calbindin-positive ureteric epithelial cells in β-catenin deficient mice but expression was maintained in metanephric mesenchymal cells (Figs. 1J–L).

β-Catenin deficient mutant pups reached term but died within 24 h of birth. Dissection of newborn pups revealed bilateral renal aplasia in 43% of pups and bilateral tiny dysplastic kidney rudiments in 57% of pups (Fig. 2A, Table 1). These rudiments were characterized by histology as deficient in nephrons, collecting ducts and cortico-medullary patterning (Figs. 2B, C). To begin to define the embryologic mechanisms underlying this phenotype, we examined kidney tissue during embryogenesis. At E12.5, a stage at which mesenchymal–epithelial interactions generate ureteric branches and nephrogenic intermediate structures, no histologic abnormalities other than small kidney size were observed in β-catenin mutant mice (Fig. 2D). However, direct examination of ureteric branches by GFP fluorescence microscopy revealed a marked attenuation of branching at this stage of development (Fig. 2F). By E13.5, a dysgenetic kidney phenotype was clearly demonstrated by histology (Fig. 2E). Thus, abnormal branching in β-catenin deficient mice precedes formation of a dysgenetic kidney.

Effect of β-catenin deficiency on cell adhesion, apoptosis and proliferation

To identify possible mechanisms by which β-catenin deficiency could cause abnormal kidney development we investigated cellular mechanisms important for branching morphogenesis and controlled by β-catenin. β-Catenin functions in adherens junctions by linking E-cadherin to the actin cytoskeleton. Together, β-catenin and actin, in concert with p120-catenin, α-catenin, and E-cadherin, control the formation, maintenance and functions of adherens junctions (Hartsock and Nelson, in press; Kemler, 1993). Since β-catenin controls the expression of E-cadherin in nonrenal tissues (Jamora et al., 2003) we examined E-cadherin expression in mutant kidney tissue. Immunohistochemical analysis of epithelial tubules of β-catenin mutant and wild type kidneys revealed similar patterns of E-cadherin expression (Fig. 3A). Further, electron microscopy demonstrated that junctional complexes and adherens junctions are maintained in the epithelial cells of the ureteric bud in the β-catenin mutants (Fig. 3B).

Decreased cell survival can contribute to decreased branching morphogenesis (Dziarmaga et al., 2003). We determined whether ureteric cell apoptosis was increased in β-catenin deficient mice. Analysis of apoptosis, using TUNEL assays (Figs. 3C–F) did not reveal a significant difference in the number of apoptotic ureteric bud epithelial cells in β-catenin deficient mice at E12.5 (Fig. 3G). In contrast, metanephric mesenchyme cell apoptosis was increased 3.8-fold ($P=0.0064$) in β-catenin deficient mice (Fig. 3H), consistent with the previous demonstration that the metanephric mesenchyme undergoes apoptosis if not induced by the ureteric bud (Barasch et al., 1997).

Cell proliferation is necessary for ureteric branching morphogenesis (Maretto et al., 2003; Michael and Davies, 2004) and β-catenin controls transcription of genes that positively regulate cell proliferation including Cyclin D1 (Reya and Clevers, 2005). Qualitative analysis of cell proliferation, using an in situ BrdU incorporation assay, revealed decreased cell proliferation in both ureteric and metanephric mesenchyme cells at E12.5 (Figs. 3I, J). Quantitation of BrdU incorporation revealed a 1.7-fold decrease in ureteric bud cell proliferation in β-catenin deficient mice ($P=0.0006$) (Fig. 3K).

Together, these results demonstrate that β-catenin deficiency does not disrupt junctional complexes or increase ureteric cell

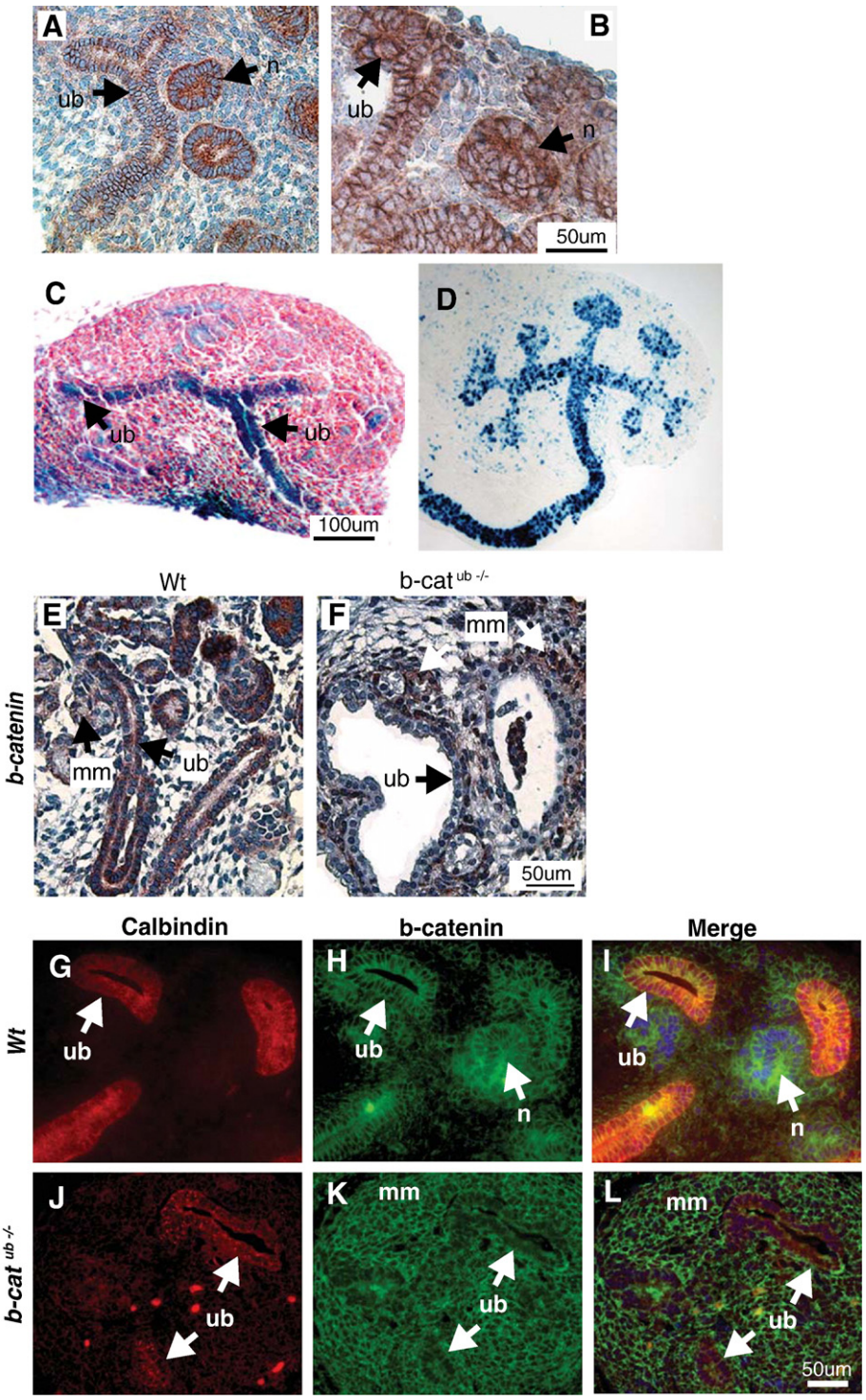

Fig. 1. β-Catenin protein expression and TCF-dependent transcriptional activity in the developing murine kidney. (A) At E13.5 β-catenin localizes to the stalks and the tips of the ureteric bud (arrow-ub), nephrogenic structures (arrow-n), and the uninduced metanephric mesenchyme. (B) A similar pattern of expression is observed at E15.5. (C) β-Catenin-dependent transcriptional activation in E11.5 TCF-gal transgenic mice. Strong X-gal staining is observed in the tips and stalks of the ureteric epithelium (arrow-ub). Low levels of staining are observed in the surrounding metanephric mesenchyme. (D) Whole mount X-gal staining of kidney tissue isolated from E12.5 BAT-gal reporter mice shows strong activity in the ureteric epithelium. (E, F) IHC demonstrating β-catenin expression in the ureteric bud at E13.5. β-Catenin is expressed in *Wt* ureteric bud tissue (arrow-ub) but is absent in β-catenin mutant tissue. Expression is maintained in the metanephric mesenchyme (white arrow-mm). (G–L) Co-localization of β-catenin and calbindin, a ureteric cell marker, in E13.5 kidney tissue. (G–I) Calbindin (red color) and β-catenin (green color) co-localize in wild type ureteric (arrow-ub) and in nephron progenitors (arrow-n). (J–L) In β-catenin mutant kidney tissue, β-catenin is not detected in calbindin-positive tubules (arrow-ub) but is expressed in metanephric mesenchyme cells (mm). ub = ureteric bud, n = nephron progenitor, mm = metanephric mesenchyme.

apoptosis. Our data demonstrates a decrease in ureteric cell proliferation that appears to be modest in size given the severity of the dysplastic phenotype in mutant mice.

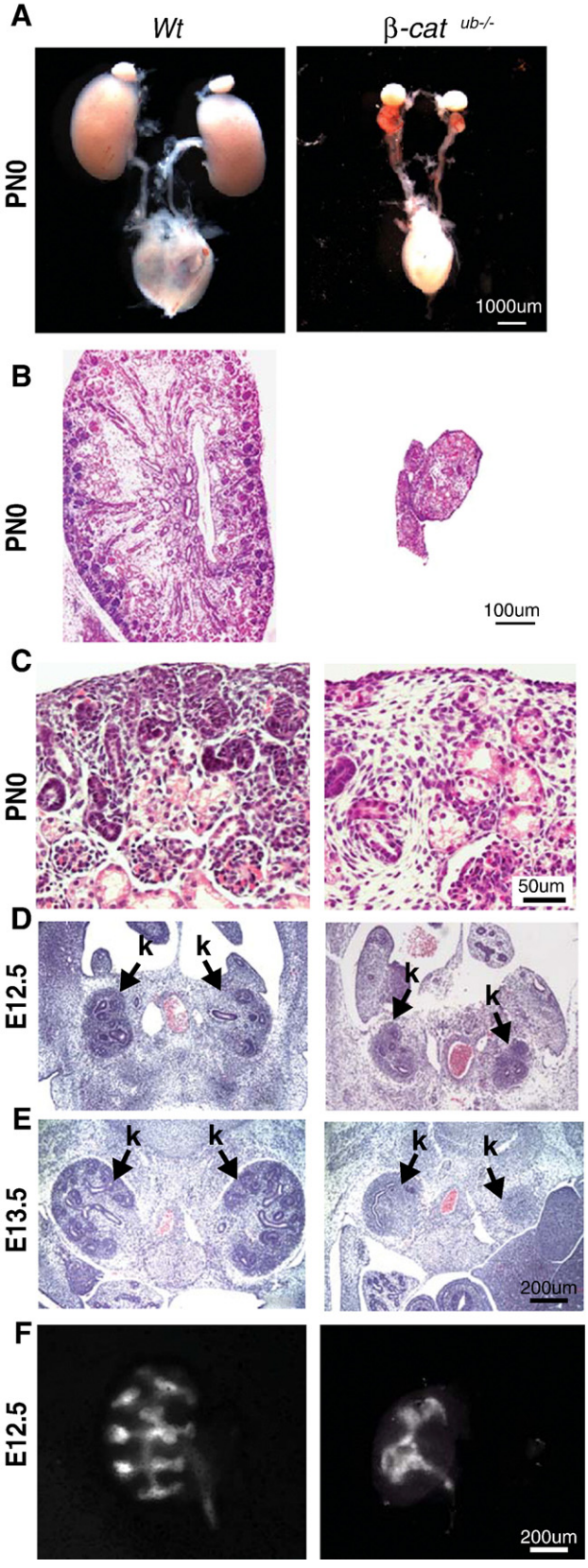

Table 1
Renal phenotypes in β-catenin deficient mice

	Mutants	Aplasia	Dysplasia
Perinatal			
Deficient	7/27 (26%)	3/7 (43%)	4/7 (57.1%)
Embryonic			
Deficient	70/287 (23.9%)	14/70 (20%)	56/70 (80%)

Kidneys were isolated from newborn mice (P0) or from pregnant females at various gestational ages. In embryos in which kidney tissue could be identified, histology was analyzed and categorized as normal or dysplastic.

Effect of β-catenin deficiency in ureteric cells on kidney mRNA expression

β-Catenin controls gene transcription in cells of diverse origin but its transcriptional targets in the embryonic kidney are largely undefined. We performed a global analysis of gene transcription in β-catenin deficient kidney tissue using the mouse genome 430 2.0 array (Affymetrix), which contains 45,000 probes sets representing over 20,000 genes. E12.5 was selected as the stage at which to perform this analysis because the branching phenotype, recognized at this stage (Fig. 4A), preceded histologic evidence of renal dysplasia. Thus, we reasoned that the changes in gene expression observed would be related more directly to changes in β-catenin expression than those observed at a later stage (e.g. E13.5) when kidney development was completely abrogated. In triplicate experiments, we compared mRNAs isolated from pools of kidneys derived from wild type and mutant mice (Fig. 4A). Analysis of the microarray data by hierarchical cluster analysis revealed a low level of variability among biological replicates (Fig. 4B), and identified 1147 differentially expressed genes (618 upregulated, 529 down regulated) between wild type and mutant kidneys using a statistical cut-off of $P<0.003$ (Fig. 4C) (Supplementary Tables 1 and 2). Microarray data was submitted to the GEO database (accession #GSE9629).

Next, we performed a gene ontology analysis to identify functional groups of differentially expressed genes. A complete list of functional categories and their accompanying genes is shown in Supplementary Table 3 and Supplementary Table 4.

Fig. 2. Renal malformation in mice with β-catenin deficiency in the ureteric cell lineage. (A) Gross anatomy of *Wt* and β-catenin deficient mice. β-Catenin deficient mice exhibit small malformed kidneys and hydroureter at P0. (B, C) H&E staining of coronal kidney sections at P0 in *Wt* and β-catenin deficient mice. In contrast to *Wt* mice, β-catenin deficient mice demonstrate very few nephron structures, an absence of cortico-medullary patterning and a lack of a nephrogenic zone. (D, E) H&E stained cross-sections of mouse embryos. (D) At E12.5 β-Catenin mutant kidneys are slightly smaller when compared to wild type kidney tissue (arrow-k) but do not demonstrate overt histologic abnormalities. (E) *Wt* kidney tissue at E13.5 is characterized by an organized array of ureteric bud tissue and developing nephrogenic structures, while β-catenin deficient kidney tissue exhibits a reduction in ureteric bud tissue and an absence of developing nephrogenic structures (arrows-k). (F) GFP fluorescence in UB branches at E12.5. Kidneys dissected from *Wt* mice demonstrate 4–5 ureteric bud branch generations while β-catenin mutants exhibit ureteric bud invasion into the surrounding mesenchyme and a highly attenuated branch pattern. k=kidney.

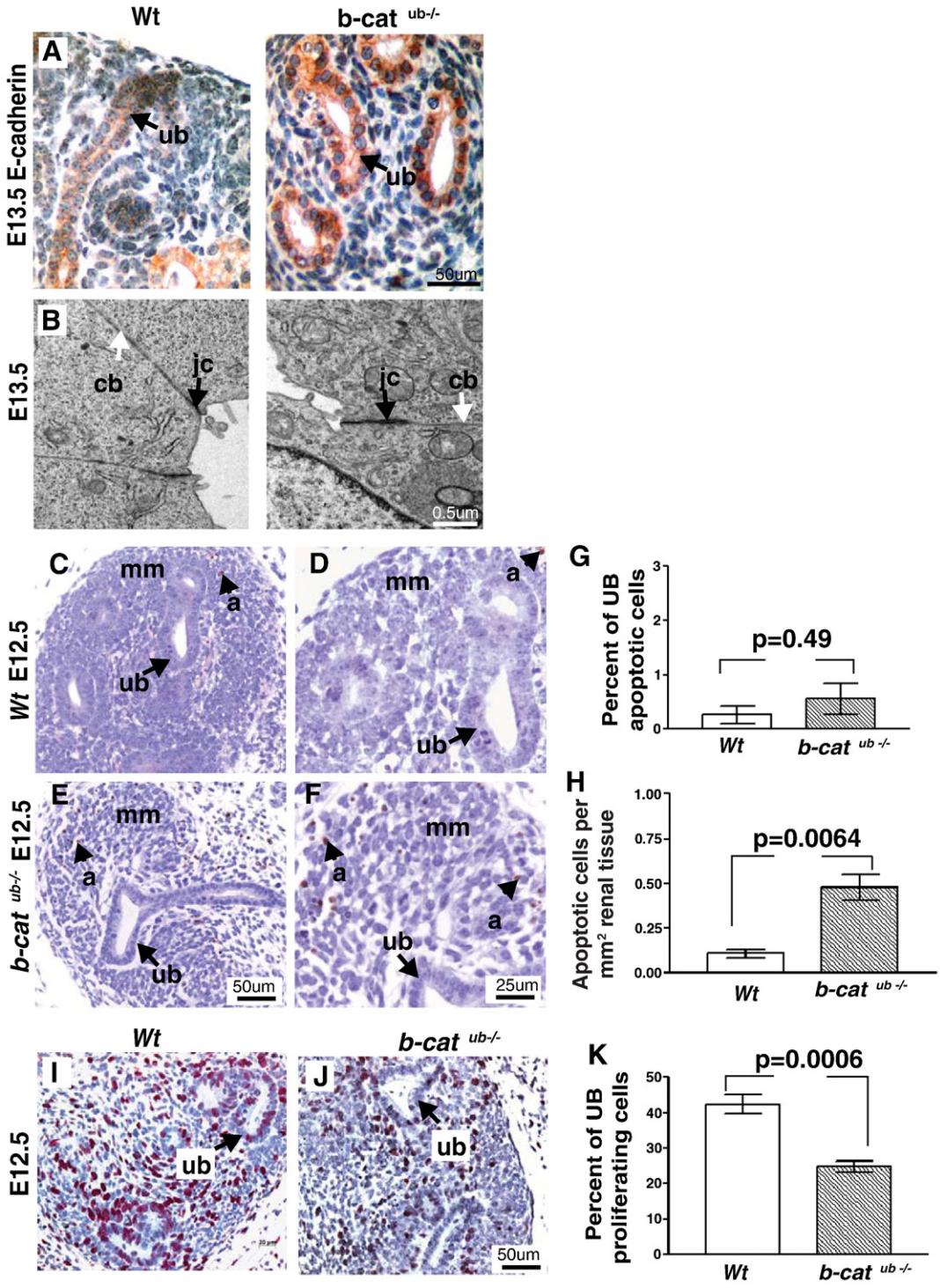

Fig. 3. Effects of β-catenin deficiency on cellular events in embryonic kidney tissue. (A) E-cadherin immunohistochemistry in E13.5 kidney tissue reveals no differences in its distribution between β-catenin deficient and wild type mice. (B) Transmission EM demonstrated normal appearing junctional complexes (black arrows-jc) and cell–cell borders (white arrows-cb) in β-catenin deficient tissue. (C–F) Analysis of apoptosis in E12.5 kidney tissue using the TUNEL assay. Brown TUNEL-positive cells (arrowhead-a) are rarely detected in the ureteric bud in *Wt* mice and β-catenin mutant mice (arrow-ub). An increase in TUNEL positive cells is observed in the mesenchyme in β-catenin mutants (mm). (G, H) Quantitative analysis of ureteric bud and mesenchymal cell apoptosis. (G) Apoptotic ureteric cells were quantified as a percentage of the total number of ureteric cells. Ureteric cell apoptosis was not significantly increased in β-catenin deficient mice (% apoptotic cells, *Wt* vs. mutant: 0.26±0.16 vs. 0.56±0.29, $P=0.49$). (H) Mesenchymal cell apoptosis, quantified as the number of apoptotic cells/mm^2 of tissue, was significantly increased in β-catenin mutant mice (*Wt* vs. mutant: 0.12±0.03 vs. 0.46±0.07, $P=0.0064$). (I–K) Analysis of cell proliferation in E12.5 kidney tissue using an in situ BrdU incorporation assay. BrdU incorporation (red color) is decreased in ureteric cells in β-catenin deficient mice compared to *Wt* (arrow-ub). (K) Quantitative analysis of ureteric cell proliferation. Ureteric cell proliferation, quantitated as the percent of BrdU-positive ureteric cells, was decreased in β-catenin mutant tissue (% proliferating cells, *Wt* vs. mutant: 42.4±2.82 vs. 24.8±1.64, $P=0.0006$). ub=ureteric bud, jc=junctional complex, cb=cell boarders, mm=metanephric mesenchyme, a=apoptotic cell.

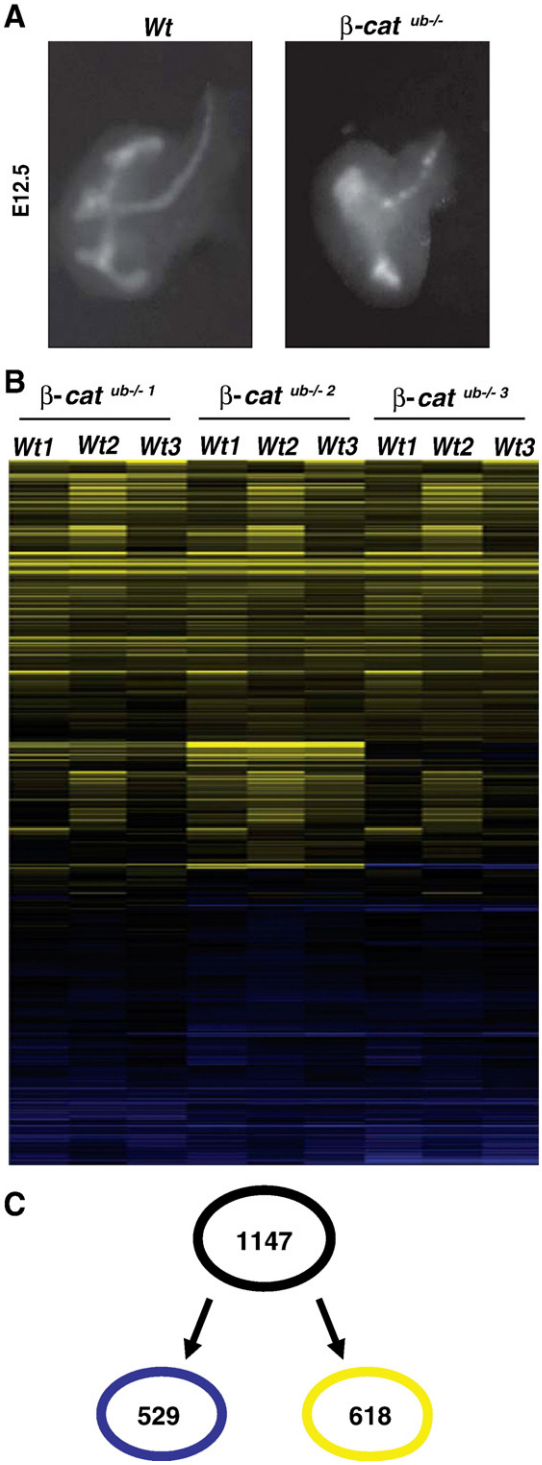

Fig. 4. Microarray array analysis of gene expression in β-catenin mutants. (A) Ureteric bud specific GFP fluorescence was used to identify the pattern of branching moprhogenesis in *Wt* and β-catenin mutant kidneys. *Wt* and β-catenin mutant kidneys were pooled to generate biological triplicates. mRNA was subjected to microarray analysis. (B) Heatmap representation of the genes differentially expressed in β-catenin mutant versus *Wt* tissue demonstrates a low level of variability among sample replicates. Each lane represents individual biological replicates normalized to each of the three *Wt* samples. (C) Analysis identified 1147 differentially expressed transcripts (618 — upregulated (yellow circle) and 529 — down regulated (blue circle)).

The subset of upregulated genes was characterized most notably for genes involved in muscle development and differentiation. Interestingly, formation of muscle is a feature of human renal dysplastic tissue (Winyard et al., 1996). Thus, we chose to further investigate myogenin, a transcription factor, which controls muscle cell differentiation. After validating increased expression of myogenin by quantitative real-time PCR (Supplemental Fig. 1), we determined its spatial expression by in situ hybridization. Our results demonstrate that increased myogenin mRNA was expressed in tissue surrounding but not within mutant kidney tissue. Thus, we conclude that microscopic contamination of kidney tissue during dissection resulted in a finding of increased expression of muscle-related genes.

Among the functional gene groups down-regulated in β-catenin mutant tissue (Supplemental Table 4) were those containing genes involved in tube morphogenesis, morphogenesis of an epithelial sheet, cell migration and metanephros development (Table 2). We inspected these categories for genes that have a functional requirement during kidney development. These genes included *Notch1*, *Pbx1*, *Gpc3*, *Wnt4*, *Jagged1*, *Wt1*, *Robo1*, and *Robo2*. Since not all differentially expressed transcripts are necessarily categorized within a gene ontology analysis, we next inspected the list of down regulated mRNA transcripts (Supplemental Table 2) for other genes that are expressed in the ureteric bud or the metanephric mesenchyme and for which a deficient state is associated with abnormal branching morphogenesis (Costantini, 2006; Piscione and Rosenblum, 2002; Shah et al., 2004; Yu et al., 2004). From these two overlapping data sets, we identified 11 down regulated genes that met these criteria (Table 3). Among these genes, *Wnt4*, *Pbx1*, *N-cam*, and *Wt1* are expressed exclusively in the mesenchyme. It is likely that abnormal branching morphogenesis in the respective deficient mice is secondary to abnormal mesenchymal development. *Robo1*, *Robo2,* and *Glypican3* are expressed in the Wolffian Duct or ureteric bud. However, genetic inactivation of each of these genes does not result in a severe phenotype resembling renal aplasia or hypodysplasia. While *Jagged1* is expressed in the ureteric bud, mutational inactivation causes a nephrogenic phenotype (Li et al., 1997). In contrast, *Lim1* and *Emx2* are both expressed in the ureteric bud and deficiency of either of these factors results in abnormal ureteric branching and renal hypoplasia. Thus, *Lim1* and *Emx2* are leading candidates for genes that could act downstream of β-catenin in the ureteric

Table 2
Gene ontology analysis, selected functional categories of genes decreased in kidney tissue of β-catenin mutant mice

GO-ID	*P*-value	Description	Genes in test set
35239	1.01e−02	Tube morphogenesis	**NOTCH1**|**PBX1**|**WNT4**|ZFHX1B|**GPC3**|CXCR4|CELSR1
2009	2.05e−02	Morphogenesis of an epithelium	**WNT4**|LAMA1|**JAG1**|ZFHX1B|CELSR1|ALDH1A3|**WT1**
1656	3.90e−02	Metanephros development	**PBX1**|**ROBO2**|**GPC3**|**WT1**
16477	3.90e−02	Cell migration	LAMA1|ALCAM|ZFHX1B|CSPG4|**ROBO2**|CXCR4|CK2|**ROBO1**|LRP6|EDNRB

Table 3
Selected mRNA transcripts significantly decreased in kidney tissue of β-catenin deficient mutant mice

Probe set ID	Gene title	Gene symbol	Log fold change	*P*-value
1450782_at	Wingless-related MMTV integration site 4	*Wnt4*	−1	0.002
1440954_at	Pre B-cell leukemia transcription factor 1	*Pbx1*	−0.9	0.002
1421106_at	Jagged 1	*Jag1*	−0.8	0.0005
1439556_at	Neural cell adhesion molecule 1	*Ncam1*	−0.8	0.0017
1419140_at	Activin receptor IIB	*Acvr2b*	−0.7	0.0002
1459453_at	Roundabout homolog 1 (Drosophila)	*Robo1*	−0.7	0.001
1450428_at	LIM homeobox protein 1	*Lhx1*	−0.6	0.0009
1446525_at	Glypican 3	*Gpc3*	−0.5	0.0005
1443221_at	Wilms tumor homolog	*Wt1*	−0.5	0.0002
1458229_at	Roundabout homolog 2 (Drosophila)	*Robo2*	−0.5	0.002
1456258_at	Empty spiracles homolog 2 (Drosophila)	*Emx2*	−0.4	0.0002

cell lineage and which are functionally required during early stages of branching morphogenesis.

We validated the results arising from our global gene expression analysis using quantitative real time PCR and in situ hybridization. Quantitative real-time PCR using mRNA isolated from E12.5 kidney tissue demonstrated a 2- and 6-fold decrease in *Emx2* and *Lim1* mRNA transcripts respectively when compared to wild type (Fig. 5A). In contrast, no change in E-cadherin mRNA expression was observed between β-catenin mutants and wild type mice (Fig. 5A), which is consistent with our analysis of E-cadherin protein expression (Figs. 3A, B). Next we used in situ hybridization to determine the spatial location of these alterations. While *Emx2* and *Lim1* mRNAs were expressed in both metanephric mesenchyme and ureteric cells in kidney tissue from wild type mice (Kobayashi et al., 2005; Miyamoto et al., 1997), the expression of each was decreased in the ureteric bud epithelium but maintained in the mesenchymal derivatives in β-catenin mutant mice (Figs. 5B, C).

Mutational inactivation of *Emx2* results in decreased mRNA expression of *Lim1*, *c-ret,* and *Pax-2* in the ureteric bud (Kobayashi et al., 2005; Miyamoto et al., 1997). Having shown a decrease in *Lim1*, we next determined the expression of *c-ret. Q*uantitative real-time PCR showed a 1.9-fold decrease in *c-ret* mRNA expression in β−catenin mutant kidney tissue. However, as in our microarray analysis, this decrease was not statistically significant (Fig. 5D). Consistent with these findings, in situ hybridization demonstrated decreased but not absent *c-ret* mRNA expression in ureteric tips (Fig. 5F). Since *Pax2* is not represented on the mouse genome 430 2.0 array, we analyzed *Pax-2* mRNA expression by quantitative real-time PCR and

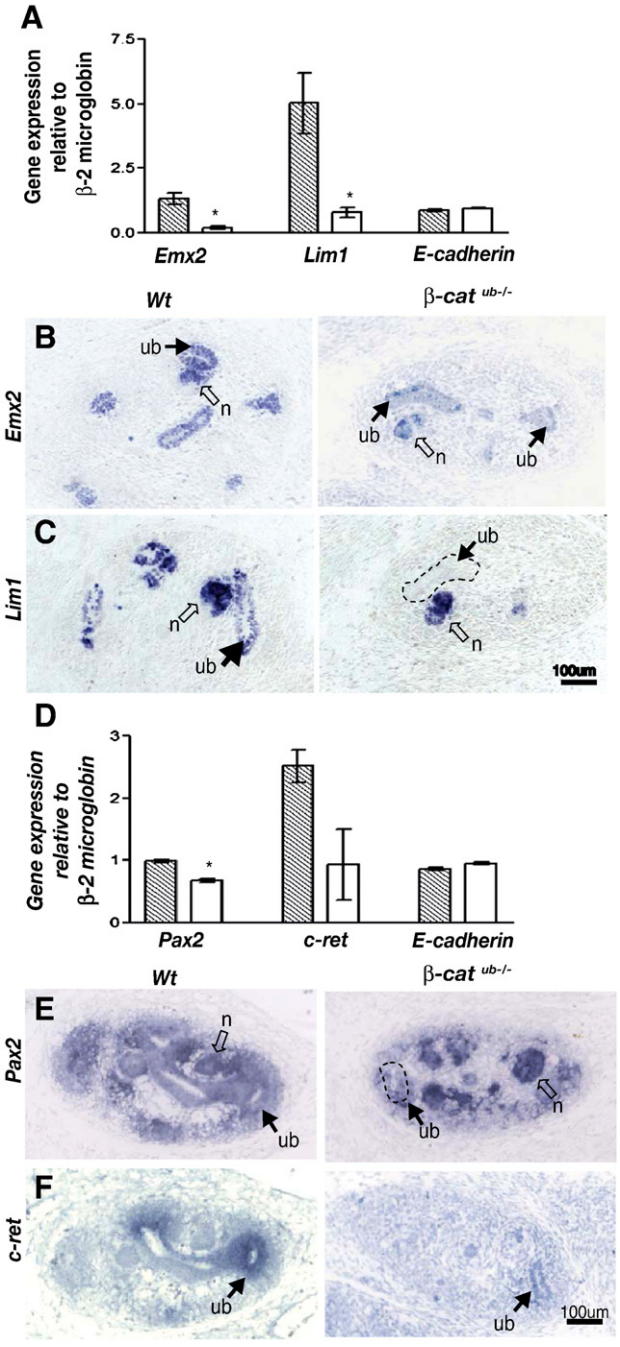

Fig. 5. Expression of kidney patterning genes in E12.5 β-catenin deficient mice. (A) Validation of microarray data by quantitative real-time PCR confirmed a significant reduction of *Emx2* (wild type vs. mutant: 1.33±0.23 vs. 0.21±0.06, $P=0.009$) and *Lim1* (wild type vs. mutant: 5.01±1.163 vs. 0.8±0.2, $P=0.02$) in β-catenin mutants. *E-cadherin* demonstrated no significant alterations when compared to *Wt* (wild type vs. mutant: 0.86±0.03 vs. 0.95±0.03, $P=0.08$). (B, C) E12.5 in situ hybridization demonstrates marked reductions in ureteric bud expression of *Emx2* (black arrow-ub) and *Lim1* (dotted black line, arrow-ub) in β-catenin mutants compared to *Wt*. These transcripts are present in the nephron progenitors (clear arrow-n). (D) Quantitative real-time PCR demonstrates decreased *Pax2* (wild type vs. mutant: 0.99±0.23 vs. 0.68±0.03, $P=0.001$) and *c-ret* (wild type vs. mutant: 2.38±0.23 vs. 1.27±0.53, $P=0.11$) mRNA transcript expression compared to *Wt*. (E) In situ hybridization demonstrates a modest decrease in *Pax2* mRNA in ureteric cells of E12.5 β-catenin mutants (dotted black line, arrow-ub) while expression is maintained in the nephron progenitors (clear arrow-n). (F) Reduced expression of *c-ret* is observed at the tips of the ureteric bud in β-catenin deficient mice compared to *Wt* (black arrow). ub=ureteric bud, n=nephron progenitor.

demonstrated a small but statistically significant 1.5-fold decrease in mRNA expression (Fig. 5D). However, in situ hybridization showed only a modest decrease in the expression of *Pax2* in the ureteric bud while expression was maintained in the mesenchyme derivatives (Fig. 5E). Yet, 24 h later, at E13.5, we could not detect *c-ret*, *Pax-2, Lim1* or *Emx2* mRNA expression in kidney ureteric bud tissue of β-catenin mutants (Fig. 6). Taken together, these results demonstrate that decreased expression of *Emx2* and *Lim1* precede decreased expression of *c-ret and Pax-2* in β-catenin mutant mice.

Ureteric branching is dependent on the establishment of distinct identities by tip and stalk cells. It has been suggested that RET-signaling participates in distinguishing tip cells from the ureteric stalk epithelium (Shakya et al., 2005). The expression of *Wnt11* in ureteric tips is dependent on *c-ret* signaling (Pepicelli et al., 1997). In turn, *Wnt11* promotes *Gdnf* expression supporting the proposition that *Wnt11* and *Gdnf* participate in an autoregulatory loop that promotes branching (Majumdar et al., 2003). In situ hybridization of E13.5 kidney tissue demonstrated near absence of *Gdnf* expression in the metanephric mesenchyme and absent *Wnt11* expression in ureteric tips in β-catenin mutant kidney tissue (Figs. 7A, B). These studies combined with loss of *c-ret* expression suggest a loss of ureteric bud tip cell fate. To investigate this possibility further, we incubated *Wt* and β-catenin mutant kidney tissue with DBA-lectin which normally binds to ureteric stalk epithelium but not to tip epithelial cells (Michael et al., 2007). In *Wt* mice DBA-lectin bound to ureteric bud stalks, but rarely to tip cells (Figs. 7C, D). In contrast, in β-catenin mutant kidney tissue DBA-lectin bound to the majority of ureteric tip cells (Figs. 7C, D). Taken together, these results demonstrate that in ureteric cells β-catenin controls expression of genes that control the attainment of a 'tip' cell fate.

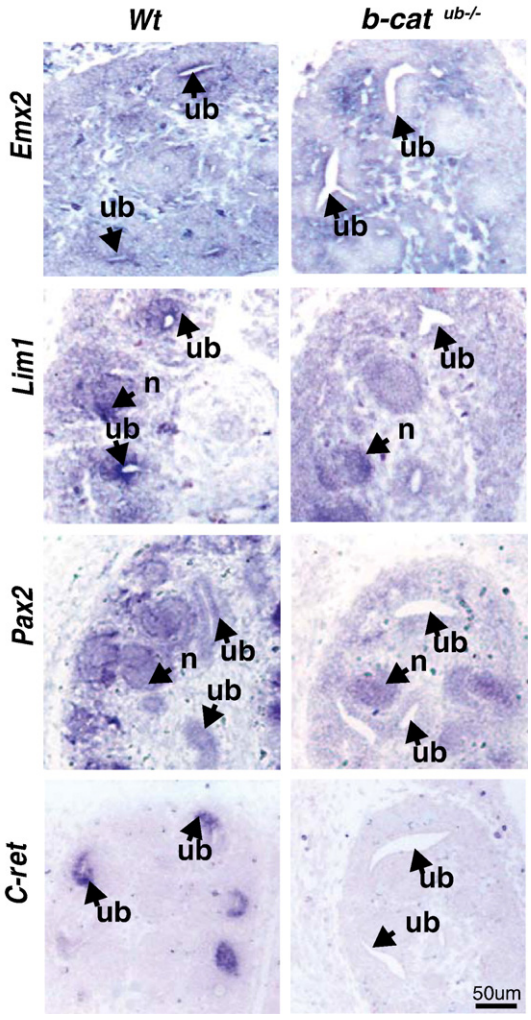

Fig. 6. Expression of kidney patterning genes in E13.5 β-catenin deficient mice. In situ hybridization demonstrates expression of *Emx2*, *Lim1*, *Pax2* and *c-ret* mRNAs in *Wt* kidney tissues. In contrast, these mRNA transcripts are not detected in ureteric cells within kidneys of β-catenin mutants (black arrows-ub). ub = ureteric bud, n = nephron progenitor.

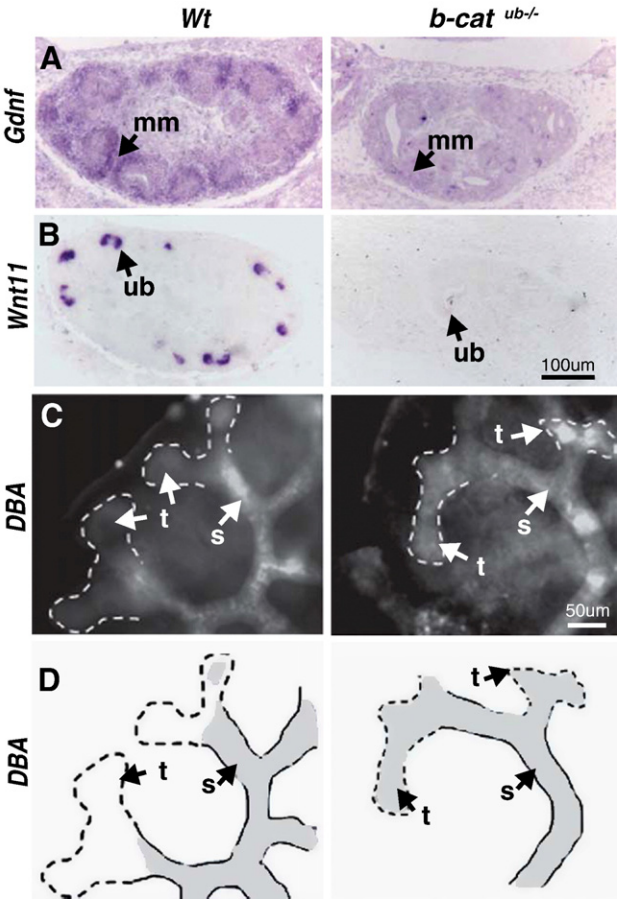

Fig. 7. Loss of ureteric tip identity in β-catenin mutants at E12.5. (A) In situ hybridization demonstrates *Gdnf* is absent from the metanephric mesenchyme surrounding the ureteric bud tips in β-catenin mutants (black arrow-mm). (B) In situ hybridization for *Wnt11* demonstrates expression in ureteric tip cells (black arrow-ub) in *Wt* mice but expression is absent in β-catenin mutant tissue (arrow-ub). (C) In *Wt* kidney tissue, DBA-lectin localizes to the ureteric bud stalk (arrow-s) but is largely excluded from the tips (arrow-t). In β-catenin deficient mice DBA-lectin expression is observed in the tips (dotted white line, arrow-t) of the ureteric bud epithelium as well as the stalks (arrow-s). (D) Schematic representation highlighting the expression pattern of DBA-lectin in *Wt* and β-catenin mutant kidney tissue. The grey color indicates DBA expression. The tips and stalks are marked as in panel C. mm = metanephric mesenchyme, ub = ureteric bud, s = stalk of the ureteric bud, t = tip of the ureteric bud.

Discussion

Renal branching morphogenesis is dependent on reciprocal epithelial–mesenchymal tissue interactions between the ureteric bud and the metanephric mesenchyme. Several members of the WNT family of secreted glycoproteins are expressed in the developing kidney in a spatial and temporal pattern consistent with a role in renal epithelial–mesenchymal interactions. However, the respective roles of canonical versus non-canonical Wnt signaling during branching morphogenesis in vivo has not been defined. Here, we demonstrate that branching morphogenesis is dependent on expression of β-catenin in the ureteric epithelium. Absence of ureteric cell β-catenin expression causes decreased expression of *Emx2* and *Lim1* in ureteric cells. These changes in ureteric cell gene expression are followed by decreased expression of *Pax-2, c-ret, Wnt11, and Gdnf* and a subsequent loss of ureteric cell tip identity. Together, these results demonstrate that canonical WNT signaling controls a hierarchy of gene expression required for branching morphogenesis.

Our results are consistent with previous reports, which implicate WNT signaling in renal branching morphogenesis. Mice deficient in *Wnt11* demonstrate renal hypoplasia and reduced ureteric bud branching (Majumdar et al., 2003). Interestingly, our phenotype is much more severe than that observed in *Wnt11* knockout mice. We believe this difference in severity may be explained by Wnt11 signaling via the non canonical planar cell polarity pathway as observed in zebrafish and Xenopus (Heisenberg et al., 2000; Smith et al., 2000). Our finding of β-catenin/TCF dependent reporter activity in the ureteric bud suggested that canonical β-catenin mediated WNT signaling could play a functional role during renal branching morphogenesis. Recent studies in in vitro models of kidney development support such a role. Inhibition of canonical WNT signaling with the WNT inhibitor Dickkopf-1 resulted in a decrease in ureteric

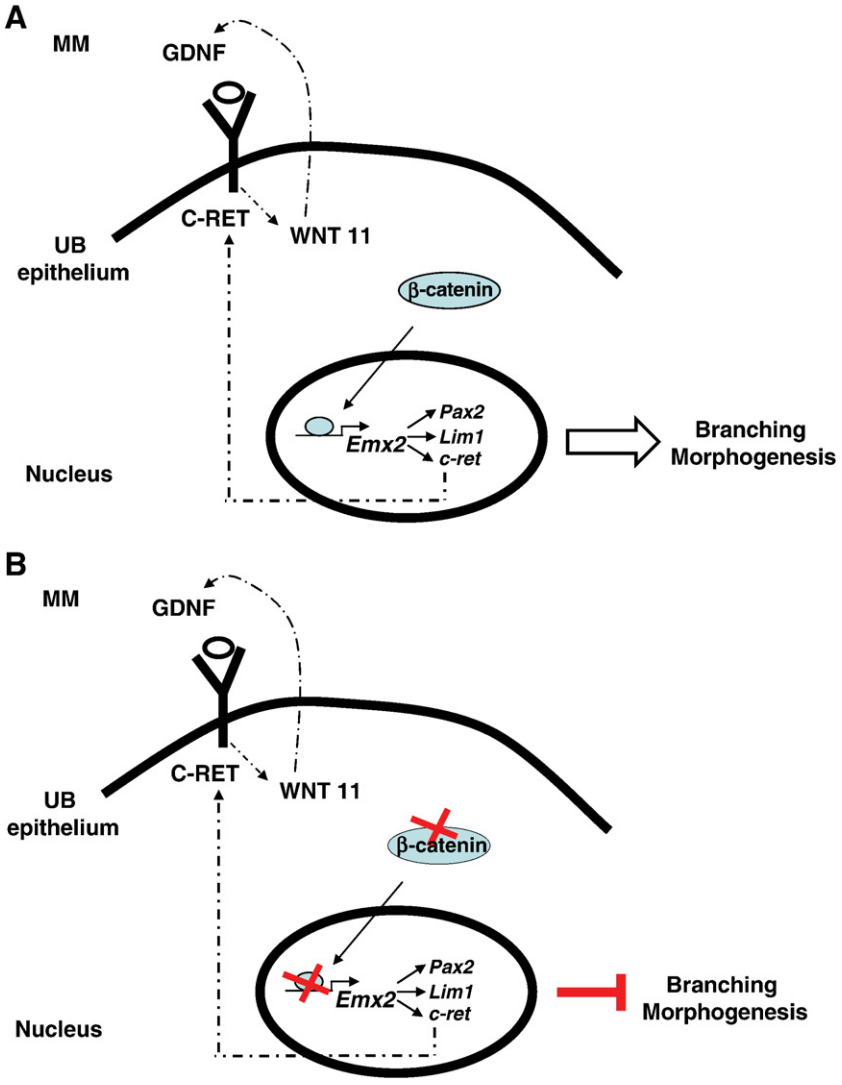

Fig. 8. Model of β-catenin function in the ureteric bud epithelium during renal branching morphogenesis. (A) β-Catenin translocates to the nucleus and partners with members of the TCF family to positively regulate *Emx2* gene transcription. *Emx2* acts up stream of *Pax2*, *Lim1* and *c-ret*. In turn the GDNF/RET/WNT11 positive feedback loop promotes branching morphogenesis. (B) β-Catenin deficiency results in a loss of *Emx2* and decreased expression of down stream factors *Pax2, Lim1 and c-ret*. Subsequent loss of *c-ret* results in a disruption of the GDNF/RET/WNT11 feedback loop, a loss of tip cell fate, and arrest of branching morphogenesis.

branching (Iglesias et al., 2007). Genetic studies identified Pygopus (Pygo) as a component of the WNT signaling pathway which interacts with β-catenin during the accumulation and formation of the β-catenin transcriptional complex. Compound mouse mutants for *pygo1* and *pygo2,* which demonstrate a reduction in canonical Wnt signaling, demonstrated expanded ureteric bud tips and reduced tip density, thus indicating a potential role for canonical Wnt signaling during renal branching morphogenesis (Schwab et al., 2007).

The multi-functional roles of β-catenin in cell–cell adhesion and gene transcription suggested several possible cellular mechanisms by which β-catenin deficiency could cause renal agenesis or malformation. Our analysis of E-cadherin expression and junctional complex structure provided no evidence to suggest that β-catenin deficiency interrupts the adherens complex. Similarly, knockdown of β-catenin in lacrimal gland and lung has no effect on adherens junctions (Dean et al., 2005). These observations are consistent with those in other conditional models of β-catenin deficiency showing a compensatory increase of γ-catenin in cardiomyocytes (Zhou et al., 2007) and of plakoglobulin in early stage embryos (Huelsken et al., 2000). β-catenin also controls genes that modulate the cell cycle. During renal branching morphogenesis, cell proliferation is spatially regulated with proliferative rates at branching tips exceeding that in growing trunks (Michael and Davies, 2004). Our results, which demonstrate a modest decrease in cell proliferation in ureteric branches in β-catenin deficient mice are consistent with the known function of β-catenin but do not completely account for the severity of the branching phenotype.

We have elucidated molecular mechanisms that could control renal malformation in β-catenin deficient mice. Our whole genome analysis of mRNA expression at an early stage of renal dysgenesis demonstrated decreased expression of *Emx2* and *Lim1*. *Lim1*, a member of the LIM-class homeodomain transcription factors, is expressed in the tips of the ureteric bud. Mice deficient in *Lim1* display hypoplastic kidneys, a reduced number of glomeruli and reduced expression of *c-ret*. However, *Pax2* and *Wnt 11* expression is not altered (Kobayashi et al., 2005). *Emx2*, a homeobox transcription factor, is expressed in the Wolffian duct and ureteric bud at E11.5 and subsequently is expressed in the branching ureteric bud and developing nephron structures. In *Emx2* deficient mice, the ureteric bud invades the metanephric mesenchyme. However, ureteric bud branching is abrogated as is expression of *Pax2*, *Lim1* and *c-ret* (Miyamoto et al., 1997). The morphologic and molecular kidney phenotype we observe in β-catenin deficient mice is similar to that observed in *Emx2* mutants, suggesting control of *Emx2* by β-catenin. Indeed, TCF consensus sequences are present in the *Emx2* promoter and *Emx2* is a target of canonical WNT signaling in the dorsal telecephalon (Theil et al., 2002) and in the mesenchyme of the rat kidney (Schmidt-Ott et al., 2007). In contrast to *Emx2* null mice, mice with β-catenin deficiency targeted only to ureteric cells do not demonstrate a total absence of *Emx2* expression in ureteric branches at E12.5. This may be due to control of *Emx2* transcription by other signaling effectors including Sonic Hedgehog and Bone Morphogenetic Proteins, as has been observed in nonrenal tissues (Theil et al., 1999; Theil et al., 2002).

Our results provide a basis for a model in which the canonical WNT/β-catenin pathway contributes to the control of patterning and branching of the ureteric epithelium (Fig. 8). In wild type kidneys, β-catenin localizes and is transcriptionally active in ureteric epithelium, while *Emx2* is active in the ureteric buds. *Emx2* regulates a genetic program involving *Lim1*, *Pax 2*, *c-ret and Wnt11* which leads to maintenance of tip cells and branching morphogenesis. In response to a loss of β-catenin the expression of *Emx2* is decreased and the downstream genes *Lim1 and Pax2* are disrupted. In turn this leads to a decrease in *c-ret* expression, a decrease in C-RET signaling, and a loss of *Wnt11*. Consequently, ureteric tip identity is lost thereby disrupting ureteric branching.

Acknowledgments

We thank Lin Chen for expert technical support and Professor Irma Thesleff (University of Helsinki) for BAT-gal reporter mice. This work was supported by a Kidney Foundation of Canada Fellowship Award (to DB), operating grants awarded by the Canadian Institutes of Health Research and the Kidney Foundation of Canada (to NDR), a Canada Research Chair (to NDR).

Appendix A. Supplementary data

Supplementary data associated with this article can be found, in the online version, at doi:10.1016/j.ydbio.2008.02.010.

References

Barasch, J., Qiao, J., McWilliams, G., Chen, D., Oliver, J.A., Herzlinger, D., 1997. Ureteric bud cells secrete multiple factors, including bFGF, which rescue renal progenitors from apoptosis. Am. J. Physiol. 273, F757–F767.

Brault, V., Moore, R., Kutsch, S., Ishibashi, M., Rowitch, D.H., McMahon, A.P., Sommer, L., Boussadia, O., Kemler, R., 2001. Inactivation of the beta-catenin gene by Wnt1-Cre-mediated deletion results in dramatic brain malformation and failure of craniofacial development. Development 128, 1253–1264.

Cano-Gauci, D.F., Song, H.H., Yang, H., McKerlie, C., Choo, B., Shi, W., Pullano, R., Piscione, T.D., Grisaru, S., Soon, S., Sedkackova, L., Tanswell, A.K., Mak, T.W., Yeger, H., Lockwood, G.A., Rosenblum, N., Filmus, J., 1999. Glypican-3-deficient mice exhibit the overgrowth and renal abnormalities typical of the Simpson–Golabi–Behmel syndrome. J. Cell Biol. 146, 255–264.

Cheon, S.S., Cheah, A.Y., Turley, S., Nadesan, P., Poon, R., Clevers, H., Alman, B.A., 2002. beta-Catenin stabilization dysregulates mesenchymal cell proliferation, motility, and invasiveness and causes aggressive fibromatosis and hyperplastic cutaneous wounds. Proc. Natl. Acad. Sci. U. S. A. 99, 6973–6978.

Costantini, F., 2006. Renal branching morphogenesis: concepts, questions, and recent advances. Differentiation 74, 402–421.

Dean, C.H., Miller, L.A., Smith, A.N., Dufort, D., Lang, R.A., Niswander, L.A., 2005. Canonical Wnt signaling negatively regulates branching morphogenesis of the lung and lacrimal gland. Dev. Biol. 286, 270–286.

Dziarmaga, A., Clark, P., Stayner, C., Julien, J.P., Torban, E., Goodyer, P., Eccles, M., 2003. Ureteric bud apoptosis and renal hypoplasia in transgenic PAX2-Bax fetal mice mimics the renal–coloboma syndrome. J. Am. Soc. Nephrol. 14, 2767–2774.

Godin, R.E., Takaesu, N.T., Robertson, E.J., Dudley, A.T., 1998. Regulation of

BMP7 expression during kidney development. Development 125, 3473–3482.
Hartsock, A., Nelson, W.J., in press. Adherens and tight junctions: structure, function and connections to the actin cytoskeleton. Biochim. Biophys. Acta. doi:10.1016/j.bbamem.2007.07.012.
Heisenberg, C.P., Tada, M., Rauch, G.J., Saude, L., Concha, M.L., Geisler, R., Stemple, D.L., Smith, J.C., Wilson, S.W., 2000. Silberblick/Wnt11 mediates convergent extension movements during zebrafish gastrulation. Nature 405, 76–81.
Hochberg, Y., Benjamini, Y., 1990. More powerful procedures for multiple significance testing. Stat. Med. 9, 811–818.
Hu, M.C., Piscione, T.D., Rosenblum, N.D., 2003. Elevated Smad1/b-catenin molecular complexes and renal medullary cystic dysplasia in ALK3 transgenic mice. Development 130, 2753–2766.
Huelsken, J., Behrens, J., 2002. The Wnt signalling pathway. J. Cell Sci. 115, 3977–3978.
Huelsken, J., Vogel, R., Brinkmann, V., Erdmann, B., Birchmeier, C., Birchmeier, W., 2000. Requirement for beta-catenin in anterior–posterior axis formation in mice. J. Cell Biol. 148, 567–578.
Iglesias, D.M., Hueber, P.A., Chu, L., Campbell, R., Patenaude, A.M., Dziarmaga, A.J., Quinlan, J., Mohamed, O., Dufort, D., Goodyer, P.R., 2007. Canonical WNT signaling during kidney development. Am. J. Physiol.: Renal Physiol. 293, F494–F500.
Jamora, C., DasGupta, R., Kocieniewski, P., Fuchs, E., 2003. Links between signal transduction, transcription and adhesion in epithelial bud development. Nature 422, 317–322.
Kemler, R., 1993. From cadherins to catenins: cytoplasmic protein interactions and regulation of cell adhesion. Trends Genet. 9.
Kobayashi, A., Kwan, K.M., Carroll, T.J., McMahon, A.P., Mendelsohn, C.L., Behringer, R.R., 2005. Distinct and sequential tissue-specific activities of the LIM-class homeobox gene Lim1 for tubular morphogenesis during kidney development. Development 132, 2809–2823.
Kress, C., Vogels, R., De Graaff, W., Bonnerot, C., Meijlink, F., Nicolas, J.-F., Deschamps, J., 1990. Hox-2.3 upstream sequences mediate lacZ expression in intermediate mesoderm derivatives of transgenic mice. Development 109, 775–786.
Kuure, S., Sainio, K., Vuolteenaho, R., Ilves, M., Wartiovaara, K., Immonen, T., Kvist, J., Vainio, S., Sariola, H., 2005. Crosstalk between Jagged1 and GDNF/Ret/GFRalpha1 signalling regulates ureteric budding and branching. Mech. Dev. 122, 765–780.
Li, L., Krantz, I.D., Deng, Y., Genin, A., Banta, A.B., Collins, C.C., Qi, M., Trask, B.J., Kuo, W.L., Cochran, J., Costa, T., Pierpont, E.M., Rand, E.B., Piccoli, D.A., Hood, L., Spinner, N.B., 1997. Alagille syndrome is caused by mutations in human Jagged1, which encodes a ligand for Notch 1. Nat. Genet. 16, 243–251.
Maere, S., Heymans, K., Kuiper, M., 2005. BiNGO: a Cytoscape plugin to assess overrepresentation of gene ontology categories in biological networks. Bioinformatics 21, 3448–3449.
Majumdar, A., Vainio, S., Kispert, A., McMahon, J., McMahon, A.P., 2003. Wnt11 and Ret/Gdnf pathways cooperate in regulating ureteric branching during metanephric kidney development. Development 130, 3175–3185.
Maretto, S., Cordenonsi, M., Dupont, S., Braghetta, P., Broccoli, V., Hassan, A.B., Volpin, D., Bressan, G.M., Piccolo, S., 2003. Mapping Wnt/beta-catenin signaling during mouse development and in colorectal tumors. Proc. Natl. Acad. Sci. U. S. A. 100, 3299–3304.
Mendelsohn, C., Batourina, E., Fung, S., Gilbert, T., Dodd, J., 1999. Stromal cells mediate retinoid-dependent functions essential for renal development. Development 126, 1139–1148.
Michael, L., Davies, J.A., 2004. Pattern and regulation of cell proliferation during murine ureteric bud development. J. Anat. 204, 241–255.
Michael, L., Sweeney, D.E., Davies, J.A., 2007. The lectin Dolichos biflorus agglutinin is a sensitive indicator of branching morphogenetic activity in the developing mouse metanephric collecting duct system. J. Anat. 210, 89–97.
Miyamoto, N., Yoshida, M., Kuratani, S., Matuso, I., Aizawa, S., 1997. Defects of urogenital development in mice lacking Emx2. Development 124, 1653–1664.
Moriyama, A., Kii, I., Sunabori, T., Kurihara, S., Takayama, I., Shimazaki, M., Tanabe, H., Oginuma, M., Fukayama, M., Matsuzaki, Y., Saga, Y., Kudo, A., 2007. GFP transgenic mice reveal active canonical Wnt signal in neonatal brain and in adult liver and spleen. Genesis 45, 90–100.
Nusse, R., 2005. Wnt signaling in disease and in development. Cell Res. 15, 28–32.
Park, J.S., Valerius, M.T., McMahon, A.P., 2007. Wnt/beta-catenin signaling regulates nephron induction during mouse kidney development. Development 134, 2533–2539.
Pepicelli, C.V., Kispert, A., Rowitch, D., McMahon, A.P., 1997. GDNF induces branching and increased cell proliferation in the ureter of the mouse. Dev. Biol. 192, 193–198.
Piscione, T.D., Rosenblum, N.D., 2002. The molecular control of renal branching morphogenesis: current knowledge and emerging insights. Differentiation 70, 227–246.
Reya, T., Clevers, H., 2005. Wnt signalling in stem cells and cancer. Nature 434, 843–850.
Saxen, L., 1987. Organogenesis of the Kidney. Cambridge Univ. Press, Cambridge.
Schmidt-Ott, K.M., Masckauchan, T.N., Chen, X., Hirsh, B.J., Sarkar, A., Yang, J., Paragas, N., Wallace, V.A., Dufort, D., Pavlidis, P., Jagla, B., Kitajewski, J., Barasch, J., 2007. beta-catenin/TCF/Lef controls a differentiation-associated transcriptional program in renal epithelial progenitors. Development 134, 3177–3190.
Schwab, K.R., Patterson, L.T., Hartman, H.A., Song, N., Lang, R.A., Lin, X., Potter, S.S., 2007. Pygo1 and Pygo2 roles in Wnt signaling in mammalian kidney development. BMC Biol. 5, 15.
Shah, M.M., Sampogna, R.V., Sakurai, H., Bush, K.T., Nigam, S.K., 2004. Branching morphogenesis and kidney disease. Development 131, 1449–1462.
Shakya, R., Watanabe, T., Costantini, F., 2005. The role of GDNF/Ret signaling in ureteric bud cell fate and branching morphogenesis. Dev. Cell 8, 65–74.
Shannon, P., Markiel, A., Ozier, O., Baliga, N.S., Wang, J.T., Ramage, D., Amin, N., Schwikowski, B., Ideker, T., 2003. Cytoscape: a software environment for integrated models of biomolecular interaction networks. Genome Res. 13, 2498–2504.
Smith, J.C., Conlon, F.L., Saka, Y., Tada, M., 2000. Xwnt11 and the regulation of gastrulation in Xenopus. Philos. Trans. R Soc. Lond., B Biol. Sci. 355, 923–930.
Srinivas, S., Goldberg, M.R., Watanabe, T., D'Agati, V., Al-Awqati, Q., Costantini, F., 1999. Expression of green fluorescent protein in the ureteric bud of transgenic mice: a new tool for the analysis of ureteric bud morphogenesis. Dev. Genet. 24, 241–251.
Theil, T., Alvarez-Bolado, G., Walter, A., Ruther, U., 1999. Gli3 is required for Emx gene expression during dorsal telencephalon development. Development 126, 3561–3571.
Theil, T., Aydin, S., Koch, S., Grotewold, L., Ruther, U., 2002. Wnt and Bmp signalling cooperatively regulate graded Emx2 expression in the dorsal telencephalon. Development 129, 3045–3054.
Vainio, S., Lin, Y., 2002. Coordinating early kidney development: lessons from gene targeting. Nat. Rev., Genet. 3, 533–543.
Winyard, P.J.D., Nauta, J., Lirenman, D.S., Hardman, P., Sams, V.R., Risdon, R.A., Woolf, A.S., 1996. Deregulation of cell survival in cystic and dysplastic renal development. Kidney Int. 49, 135–146.
Yu, J., McMahon, A.P., Valerius, M.T., 2004. Recent genetic studies of mouse kidney development. Curr. Opin. Genet. Dev. 14, 550–557.
Zhao, H., Kegg, H., Grady, S., Truong, H.T., Robinson, M.L., Baum, M., Bates, C.M., 2004. Role of fibroblast growth factor receptors 1 and 2 in the ureteric bud. Dev. Biol. 276, 403–415.
Zhou, J., Qu, J., Yi, X.P., Graber, K., Huber, L., Wang, X., Gerdes, A.M., Li, F., 2007. Upregulation of gamma-catenin compensates for the loss of beta-catenin in adult cardiomyocytes. Am. J. Physiol.: Heart Circ. Physiol. 292, H270–H276.